Bull. Soc. R. Sci. Liège, 2024, **93**(2), 623–635 *Peer-reviewed conference paper*
doi:10.25518/0037-9565.11817

Photometric Variability of Low Mass Stars and Brown Dwarfs in IC 348 and Taurus Star-Forming Regions

Samrat GHOSH[1,*], Soumen MONDAL[1,*], Santosh JOSHI[2], Sneh LATA[2] and Rajib KUMBHAKAR[1]

[1] S. N. Bose National Centre for Basic Sciences, Salt Lake, Kolkata 700106, India
[2] Aryabhatta Research Institute of Observational Sciences (ARIES), Manora Peak, Nainital-263002, India
[*] Corresponding authors: samrat687@gmail.com; soumen.mondal@bose.res.in

Paper presented at the 3rd BINA Workshop on "Scientific Potential of the Indo-Belgian Cooperation", held at the Graphic Era Hill University, Bhimtal (India), 22nd–24th March 2023.

Abstract

Low-mass stars belonging to the Mspectral type are the most numerous stars in our Galaxy, amounting to about two-thirds in number, and are found at the bottom of the main sequence in the H-R diagram. Photometric studies of low-mass stars, including brown dwarfs (BDs), provide several important evolutions of their atmosphere, magnetic flares and chromospheric activity. This paper highlights a few interesting results from our optical *I*-band observations of 2MASS J03435638+3209591 in the young star-forming IC 348 region and three BDs in Taurus star-forming regions using ground-based telescopes as well as a space-based telescope. We estimated the fast periodicities in the range of 1.5 to 3 hours in Taurus BDs. Furthermore, using the long-term photometry from the Transiting Exoplanet Survey Satellite (TESS), we have conducted a time-resolved variability analysis of CFHT-BD-Tau 4. The periodogram analysis of TESS data reveals an orbital period of ~ 3 days. We found two flare events in TESS sector 43 data for this BD and estimated the flared energies as 4.59×10^{35} erg and 2.64×10^{36} erg, which sit in the superflare range.

Keywords: star forming regions, brown dwarfs, very low mass stars, M dwarfs, Flares

1. Introduction

Very low-mass stars (VLMs) refer to the stellar and substellar objects with masses below $0.6\,M_\odot$ to the planetary limit ($0.013\,M_\odot$) (Allard et al., 1997), which include the spectral types of mid-K, M, L, and T to the coldest known brown dwarf Y (Allard et al., 2012). They extend from the edge of the hydrogen-burning main sequence (MS, i.e., mid-K and early-M) to the deuterium-burning Brown Dwarfs (BDs; mass-range 80–13 $M_{\rm J}$) with the transition at M6 spectral type at the young age of star-forming regions (SFRs) (Chabrier and Baraffe, 2000; Luhman et al., 2016). Choosing a star-forming region seems technically suitable for studying these

objects with ground-based telescopes, as their luminosities and temperatures are higher than galactic field BDs and low-mass stars. Photometric variability studies can detect periodic and aperiodic variability in young BDs and probe the nature of their atmospheres (Cody and Hillenbrand, 2014). Stable surface features like star spots or dust clouds cause non-uniformity in the surface, which causes periodic optical modulation of the flux as the object rotates. Whereas aperiodic variability is due to non-uniform accretion from disks, magnetic spots, and dynamic star spots or dust clouds, changing with time scales different from the rotation periods. VLMS, including BDs, are fast rotators with periods ranging from a few hours to days (Cody and Hillenbrand, 2010; Crossfield, 2014). The average rotation rate of stars varies across the main sequence, differing in stellar structure and magnetic properties. The periodic variability can be observed within a few nights of photometric monitoring using 1–2 m class ground-based telescopes.

We highlight here the findings of the optical I-band photometric variability of VLMs and BDs from two star-forming regions, IC 348 and Taurus. IC 348 is a young (1–3 Myr) and nearby ($\sim$ 310 pc) star-forming region in Perseus molecular cloud (Luhman et al., 2003). Because of the IC 348 cluster's intermediate star density ($\rho \simeq 100$–$500\,M_{\odot}\,\mathrm{pc}^{-3}$; Parker and Alves de Oliveira, 2017), it has enough stars ($\sim$ 500) to detect large populations of low-mass objects in 10–20 arcmin field of view (FoV), and similarly for Taurus. Our optical I-band photometric variability study down to $\sim$ 19 magnitudes in IC 348 explored the hour-scale rotation in VLMs. We present the findings of a young M dwarf 2MASS J03435638+3209591 (SpT = M7.25 V, I = 18.61) in IC 348. This BD is reported to be a possible variable source (Cody and Hillenbrand, 2014; Getman et al., 2017). BDs are generally fast rotators. This makes this object an object of interest. Moreover, deuterium burning instability or ε-mechanism is induced in the core of fully convective VLMs and BDs (Palla and Baraffe, 2005) due to the high sensitivity of nuclear energy generation rate to temperature ($\sim T^{12}$), which could give a pulsation period that varies between 1 h to 5 h, which in turn could be observed as a short periodicity in the data with observable amplitude.

We have monitored three known brown dwarfs: CFHT-BD-Tau 2 (hereafter, CT2), CFHT-BD-Tau 3 (hereafter, CT3), and CFHT-BD-Tau 4 (hereafter, CT4) (Age $\simeq$ 1 Myr; Martín et al., 2001) in Taurus Molecular clouds with different Indian national telescope facilities on various epochs. The BD nature of CT2, CT3, and CT4 has been confirmed spectroscopically (Martín et al., 2001). We also conducted a time-resolved variability analysis of CT4 using the 2-min cadence data from the Transiting Exoplanet Survey Satellite (TESS). Previous studies revealed that CT2, CT3, and CT4 have day-scale rotation periods of 2.93, 0.96, and 2.95 days, respectively (Scholz et al., 2018; Rebull et al., 2020) in K2 mission observations. Magnetic activity is common in M dwarfs, which is supported by the flaring of CT4 and previously reported H_{α} detection (Mohanty et al., 2005) for this BD. Previous studies have also shown that CT4 is accreting, but CT2 and CT3 are non-accretors (Mohanty et al., 2005).

2. Observations and Data Analysis

The *I*-band optical photometric data for 2MASS J03435638+3209591 were obtained from the 1.3-m Devasthal Fast Optical Telescope (hereafter, 1.3-m DFOT) operated by ARIES, Nainital and the 2-m Himalayan Chandra Telescope (hereafter, 2-m HCT), Ladakh operated by the Indian Institute of Astrophysics (IIA), Bangalore. Data for Taurus BDs were acquired using the 1-m Sampurnanda Telescope (hereafter, 1-m ST) and 1.3-m DFOT operated by ARIES, Nainital, and the 2-m HCT. The Wright 2K CCD with 24 μm pixel size is used in 1-m ST for acquiring the data with a field of view (FoV) of 13×13 arcmin^2 (Sagar et al. 2014). The ANDOR $2K \times 2K$ CCD in 1.3-m DFOT has a pixel size of 13.5×13.5 μm^2. A set of Johnson-Cousin B, V, R, I, and H_α circular filters are available which gives an unvignetted view of 18×18 arcmin^2. The back-end instrument used in 2-m HCT is the Himalayan Faint Object Spectrograph and Camera (HFOSC). The $2K \times 2K$ part of the detector in $2K \times 4K$ CCD having a pixel size of 15 μm and a pixel scale of 0.296 arcsec is used for imaging observations. The FoV on the $2K \times 2K$ part of CCD in the imaging mode is 10×10 arcmin^2. In all these instruments, photometric images were taken in the optical *I*-band with exposure times varying according to the night condition (see Table 1).

Optical *I*-band data reduction was performed using Image Reduction and Analysis Facility (IRAF) software. Bias, flat, and cosmic ray corrections were performed to each observed frame using standard IRAF tasks. Aperture photometry using PHOT was performed on bias and flat-corrected images to get instrumental magnitudes (*I*-band) of individual sources. We used the estimated instrumental magnitudes for each observing date to construct the time-series light curves for all sources. Following Ghosh et al. (2021), we generated the light curves using differential photometry for all sources in the CCD frames. We used the Lomb–Scargle method (LS periodogram; Lomb 1976; Scargle 1982, VanderPlas 2018) to find the significant periodicity of the data. Phase light curves have been constructed using the most significant peak. We used the Python package *'astropy'* (Astropy Collaboration et al., 2013) to bin the data.

Using our new *I*-band observations from a sample of 177 light curves of IC 348, we detected 22 young M-dwarfs, including 6 BDs. Out of 22 variables, $\sim 50\%$ show hour-scale periodic variability in the period range of 3.5–11 hours; the rest are aperiodic (Ghosh et al., 2021). Here, we presented one BD source as an example of the short rotation periodicity of a faint BD detected with ground-based observation.

Using ground-based observations' time window, we monitored three Taurus BD sources in two different framings (one framing for CT2 and CT3; another for CT4) as they are separated by a larger distance than the FoV of the attached CCD camera on the telescope. We detected and analysed ~ 200 sources for 1-m ST and 2-m HCT images for CT2 and CT3 frames and ~ 30 objects for CT4 frames, as this region is less crowded. In 1.3-m DFOT, we detected ~ 700 sources in the 18×18 arcmin^2 FoV for the CFHT 2 and CFHT 3 frames. We selected ten sources of similar magnitude from these objects' light curves. We averaged them to create an average reference light curve for each night to generate a differential light curve for the target objects and references.

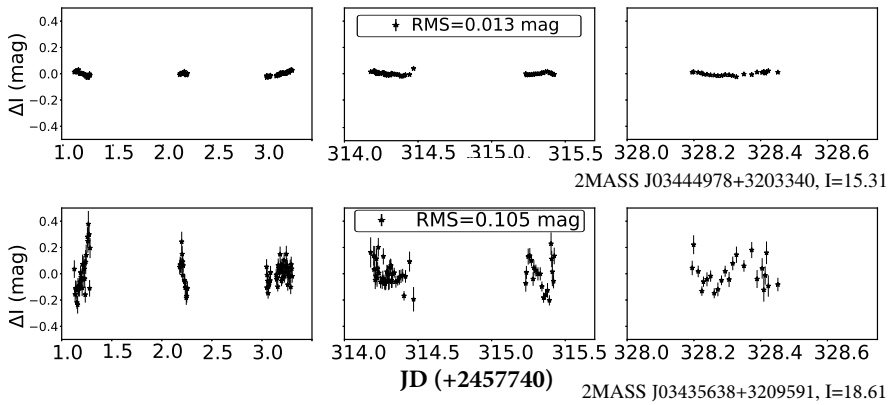

Figure 1: For example, a light curve of variable 2MASS J03435638+3209591 in the bottom left panel is shown. A non-variable reference star is shown in the top left panel. The *x*-axis is broken due to data gaps between observations. The *y*-axis is the zero-averaged *I* magnitude of the sources. Plot regenerated from Ghosh et al. (2021) with permission.

TESS observations and data analysis

The Transiting Exoplanet Survey Satellite (TESS; Ricker et al., 2015) observed CT4 with its camera 2 during sector 43 from September 16, 2021, to October 11, 2021. The four cameras of TESS as back-end instruments cover the field of view of each $24 \times 24\,\mathrm{deg}^2$ and are aligned to cover $24 \times 90\,\mathrm{deg}^2$ of the sky, which are called 'sectors' (Ricker et al., 2015). The data were stored under the Mikulski Archive for Space Telescopes (MAST) with identification number 'TIC 150058662' (TIC: TESS input catalog). We retrieved TESS data with the TIC of the object CT4 from the MAST and processed the light curves from TESS 2-min cadence data using the '*lightkurve*' package (Lightkurve Collaboration et al., 2018). We used Pre-Search Data Conditioning (PDCSAP) light curves because these are already corrected for systematic instrumental noise in the Simple Aperture Photometry (SAP) light curves. PDCSAP light curve shows short time-scale flux variation and less scatter (Smith et al., 2012; Stumpe et al., 2014).

3. Results and Discussion

The light curve of the variable object 2MASS J03435638+3209591 from IC 348 is shown in Fig. 1, showing significant variability with RMS $= 0.105$ mag.

The light curve of a non-variable source 2MASS J03444978+3203340 ($I = 15.31$) is shown in the top panel with RMS $= 0.013$ mag indicating that the object is variable. We found a short period of 4.24 hours from the LS periodogram analysis. The phase folded light curve is shown in Fig. 2.

Three light curves from three different observing nights are shown in Fig. 3 for the Taurus BDs. A few phase light curves are shown in Fig. 4. Using the LS periodogram method, we uncovered very short hour scale periodicities for all three sources ($\sim$ 1.5–3 h) from the ground-

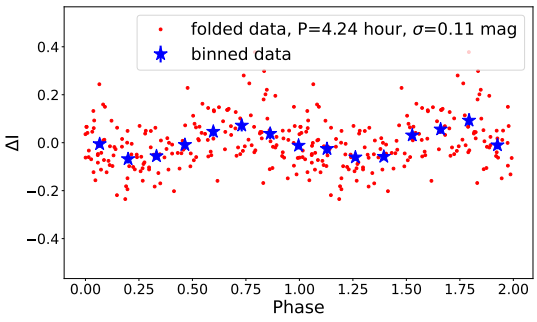

Figure 2: The phase light curve of the same periodic source with the period, $P = 4.24$ h in red dots, is shown. The blue stars represent the 15-point binned data. Plot regenerated from Ghosh et al. (2021) with permission.

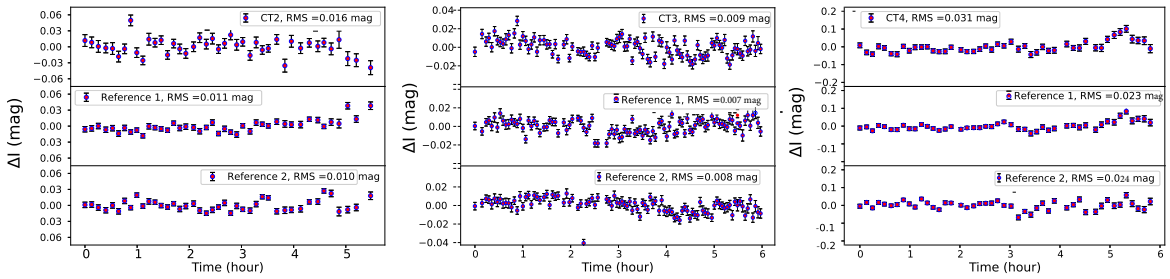

(b) CT2: 08.12.2018 - 1.3m DFOT (b) CT3: 25.12.2019 - 2m HCT (a) CT4: 30.01.2009 - 1m ST telescope

Figure 3: Three light curves of the three brown dwarfs are shown. Two non-variable reference light curves are shown in the bottom panels of each light curve. The source name, dates, and telescopes used to obtain the data are mentioned underneath each panel.

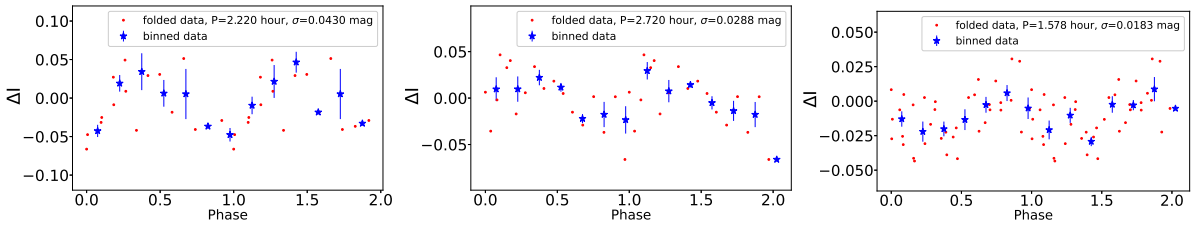

(a) CT2: 31.01.2009 - 1m ST (a) CT3: 31.01.2009 - 1m ST (a) CT4: 30.01.2009 - 1m ST telescope

Figure 4: A few example phase light curves of the BDs are shown. The blue stars represent 10-point binned data binned in phase. The source name, dates, and telescopes used to obtain the data are mentioned underneath each panel.

based *I*-band data.

Using the long-term photometry from the TESS, we have conducted a time-resolved variability analysis of CT4. The LS periodogram analysis of TESS data reveals an orbital period of ~ 2.99 days, consistent with the earlier results from the literature (2.93 days: Scholz et al. 2018 and 2.95 days: Rebull et al. 2020). The PDCSAP and normalized light curves are shown in the top left panel of Fig. 5, and the phase light curve, folded with 2.99 days, is shown in the top right panel. The red dots show the phase curve; the blue stars are binned data.

The possible explanation of the hour-scale periodicity from ground-based *I*-band data could be accretion hot spots in those BDs, co-rotating with the objects where accretion is still ongoing (Scholz and Eislöffel, 2005) and/or slowly evolving magnetic spots that create such light-curve morphology over a stable rotation period of ~ 3 days. Variable extinction from circumstellar disk can also result in either periodic or long timescale variability (Parks et al., 2014). Variable extinction might not always be sinusoidal, unlike variability caused by star spots, but might appear more likely as eclipse-like features (Parks et al., 2014). The disc's rotational speed determines extinction variations time scales, and depending on the radial distance from the star, it could range from a few hours to years (Scholz et al., 2009). If we assign the day-scale periods of CT2, CT3 and CT4 as rotational periods or due to the presence of surface spots, then another explanation of hour-scale variability could be the deuterium burning instability (Palla and Baraffe, 2005). In the mass range of 0.2 to 2.0 $M_{\odot}$, PMS stars could become pulsationally unstable during deuterium burning, which could affect the radiation and make them variable (Toma, 1972). This instability is induced in the core of fully convective BDs due to the high sensitivity of nuclear energy generation rate to temperature ($\sim T^{12}$). A small temperature perturbation could induce an order of magnitude higher energy variations causing a pulsation period between ~ 1 h to ~ 5 h and Palla and Baraffe (2005), which in turn could be observed as a short periodicity in the data with observable amplitude.

Combining this with the fact that the sources have reported day-scale periods, we could infer that the noise from ground-based monitoring may be high enough to mimic this as a periodic signal in short-time scales (hours-scale). These hour-scale periods might give some insights into variability due to little-known physics, even at low significance levels. However,

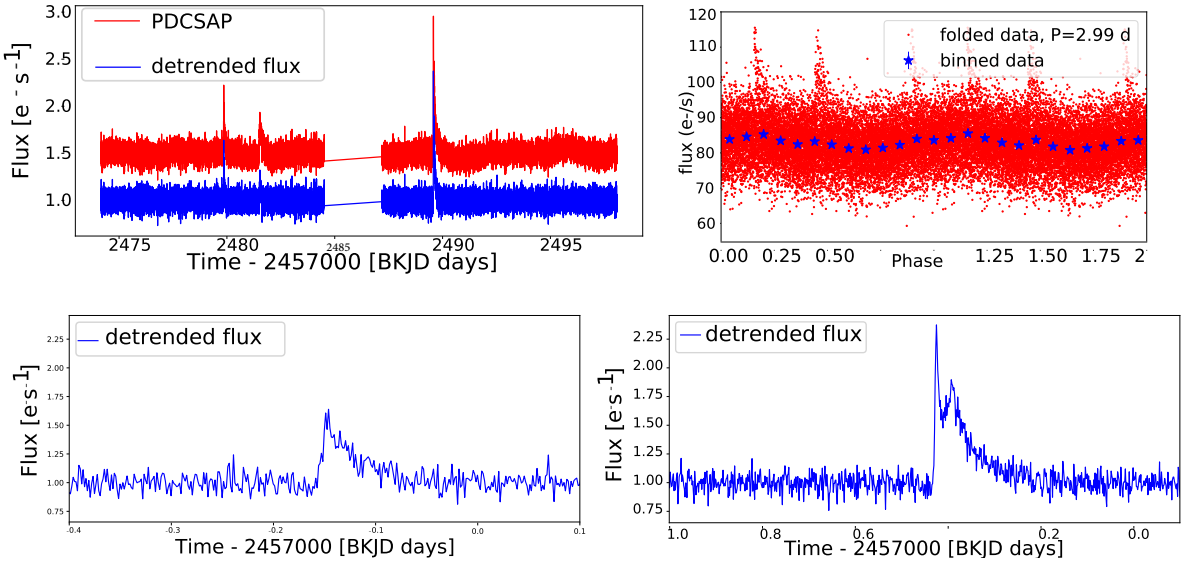

Figure 5: (*Upper left*) Corrected light curves of CFHT-BD-Tau 4 from sector 43 of TIC 150058662 2-min cadence data. The x-axis is the time in Barycentric Kepler Julian Days (BKJD), and the y-axis is the normalized TESS flux (e^-/s). Red highlights PDCSAP data; blue gives the detrended flux (e^-/s) with no intrinsic variation present. (*Upper right*) Phase light curve of CFHT-BD-Tau 4 folded with the period, $P = 2.99$ days. The red dots show the phase curve; the blue stars are binned data. The x-axis shows phase and the y-axis shows flux in (e^-/s). (*Bottom*) Zoomed-in view of the two flares.

readers should use these parameters with caution.

We analyzed the TESS sector 43 light-curve of CT4 using the '*AltaiPony*' pipeline (Ilin, 2021). '*AltaiPony*' uses `FlareLightCurve.find_flares()` to detect the flare candidates. It uses the detection criteria described in Chang et al. (2015) as outlined below. For the i-th point of a light curve, the selection criterion is given by the expressions:

$$x_i - \bar{x}_\mathrm{L} < 0 \quad (1)$$

$$\frac{|x_i - \bar{x}_\mathrm{L}|}{\sigma_\mathrm{L}} \geq N_1 \quad (2)$$

$$\frac{|x_i - \bar{x}_\mathrm{L} + w_i|}{\sigma_\mathrm{L}} > N_2 \quad (3)$$

$$ConM \geq N_3 \quad (4)$$

where the mean $\bar{x}_\mathrm{L}$ and deviation σ_L are the local statistics for a given segment, w_i is the photometric error at epoch i, and $ConM$ is the number of consecutive points which satisfy Eqns. (1) to (3). The values of $N_{1,2,3}$ are taken to be 3, 2, and 3, respectively.

We used the Savitzky-Golay filter (Savitzky and Golay, 1964) to the PDCSAP light curve for detrending any long-term periodicity. The `find_flares()` function is used to detect the flare in the detrended light curve. It gives flare duration, starting and ending time of the flare,

and equivalent duration (ED) for the detected flare. We found two flares and estimated the flare energy using the bolometric flare luminosity of 5.4×10^{32} erg for $A_v = 6.37$ (Paudel et al., 2018). We estimated the flare energies as 2.64×10^{36} erg and 4.59×10^{35} erg following the flare energy calculation method described in (Paudel et al., 2018; Ghosh et al., 2021). We summarised the properties of the flares in Table 2. The PDCSAP and normalized light curves (Fig. 5, top left panel) show two spikes indicating the flares.

4. Summary

1. The light curve of the variable object 2MASS J03435638+3209591 from IC 348 shows significant variability with RMS $= 0.105$ mag with a short period of 4.24 hours found from the LS periodogram analysis.

2. From the *I*-band light-curve analysis of the CT2, CT3 and CT4, we detected hour-scale photometric variability using the LS periodogram method. We find that the detected periods are varied in various observing dates, ranging from 1.5 to 3 hours.

3. We find here that TESS data gives a long-term stable period of 2.99 days for CT4 in sector 43, as reported in previous studies.

4. From sector 43 of TESS 2-min cadence data of CT4, we detected two flare events with energies 4.59×10^{35} erg and 2.64×10^{36} erg, which sit in the superflare range.

Acknowledgments

This research work is supported by the S. N. Bose National Centre for Basic Sciences under the Department of Science and Technology, Govt. of India. The authors are thankful to the Joint Time Allocation Committee (JTAC) members and the staff of the 1 m-ST and 1.3 m Devasthal optical telescope operated by the Aryabhatta Research Institute of Observational Sciences (ARIES, Nainital), the HCT Time Allocation Committee (HTAC) members and the staff of the Himalayan Chandra Telescope (HCT), operated by the Indian Institute of Astrophysics (IIA, Bangalore). SG is grateful to the Department of Science and Technology (DST), Govt. of India for their Innovation in Science Pursuit for Inspired Research (INSPIRE) Fellowship scheme. This paper includes data collected with the TESS mission, obtained from the Mikulski Archive for Space Telescopes (MAST) data archive at the Space Telescope Science Institute (STScI), which is operated by the Association of Universities for Research in Astronomy, Inc., under NASA contract NAS 5-26555.

Table 1: Observation log for Taurus, where "Run-Length" is the total duration of the observation.

Date	Target	Telescope	Instrument	FoV (arcmin^2)	Run-Length (hours)	N×Exposure (sec)	Seeing (arcsec)
30/01/2009	CT4	1-m ST	2K Wright CCD	13×13	4.10	46×300	1.14
31/01/2009	CT2, CT3	1-m ST	2K Wright CCD	13×13	5.81	1×400, 17×500	1.22
23/10/2009	CT4	1-m ST	2K Wright CCD	13×13	3.19	32×300	1.03
08/12/2018	CT2, CT3	1.3-m DFOT	ANDOR 2K × 2K	18×18	5.47	3×300, 39×400	3.06
25/12/2019	CT2, CT3	2-m HCT	2K × 2K CCD	10×10	5.97	40×200, 58×180	1.61

Table 2: Flare parameters of CFHT-BD-Tau 4 in TESS sector 43

Parameters	Flare start (BKJD)	Flare stop (BKJD)	E.D. (sec)	Duration (hh:mm)	Fractional Amplitude	Energy (erg)
Flare 1	2489.571444	2489.672842	4883.7 ± 70.1	2:26	1.38	2.64×10^{36}
Flare 2	2479.849736	2479.874738	851.3 ± 37.3	0:36	0.64	4.59×10^{35}

Further Information

Authors' ORCID identifiers

0000-0003-3354-850X (Samrat GHOSH)
0000-0003-1457-0541 (Soumen MONDAL)
0009-0007-1545-854X (Santosh JOSHI)
0000-0001-9367-1580 (Sneh LATA)
0000-0001-7277-2577 (Rajib KUMBHAKAR)

Author contributions

Observational data from telescopes were collected by SG, SM, SJ and SL. The light curves and power spectrum analysis were carried out by RK, SG, and SM. The examination of the flare analysis part was performed by SG and RK. The manuscript text was prepared by SG and SM. All the authors provided input on the written draft of the manuscript, as well as the discussion and interpretation of the findings.

Conflicts of interest

The authors declare no conflict of interest.

References

Allard, F., Hauschildt, P. H., Alexander, D. R. and Starrfield, S. (1997) Model atmospheres of very low mass stars and brown dwarfs. ARA&A, 35, 137–177. https://doi.org/10.1146/annurev.astro.35.1.137.

Allard, F., Homeier, D. and Freytag, B. (2012) Models of very-low-mass stars, brown dwarfs and exoplanets. RSPTA, 370(1968), 2765–2777. https://doi.org/10.1098/rsta.2011.0269.

Astropy Collaboration, Robitaille, T. P., Tollerud, E. J., Greenfield, P., Droettboom, M., Bray, E., Aldcroft, T., Davis, M., Ginsburg, A., Price-Whelan, A. M., Kerzendorf, W. E., Conley, A., Crighton, N., Barbary, K., Muna, D., Ferguson, H., Grollier, F., Parikh, M. M., Nair, P. H., Unther, H. M., Deil, C., Woillez, J., Conseil, S., Kramer, R., Turner, J. E. H., Singer, L., Fox, R., Weaver, B. A., Zabalza, V., Edwards, Z. I., Azalee Bostroem, K., Burke, D. J., Casey, A. R., Crawford, S. M., Dencheva, N., Ely, J., Jenness, T., Labrie, K., Lim, P. L., Pierfederici, F., Pontzen, A., Ptak, A., Refsdal, B., Servillat, M. and Streicher, O. (2013) Astropy: A community Python package for astronomy. A&A, 558, A33. https://doi.org/10.1051/0004-6361/201322068.

Chabrier, G. and Baraffe, I. (2000) Theory of low-mass stars and substellar objects. ARA&A, 38, 337–377. https://doi.org/10.1146/annurev.astro.38.1.337.

Chang, S. W., Byun, Y. I. and Hartman, J. D. (2015) Photometric study on stellar magnetic activity. I. Flare variability of red dwarf stars in the open cluster M37. ApJ, 814(1), 35. https://doi.org/10.1088/0004-637X/814/1/35.

Cody, A. M. and Hillenbrand, L. A. (2010) Precision photometric monitoring of very low mass σ Orionis cluster members: Variability and rotation at a few Myr. ApJS, 191(2), 389–422. https://doi.org/10.1088/0067-0049/191/2/389.

Cody, A. M. and Hillenbrand, L. A. (2014) A pulsation search among young brown dwarfs and very-low-mass stars. ApJ, 796(2), 129. https://doi.org/10.1088/0004-637X/796/2/129.

Crossfield, I. J. M. (2014) Rotation and variability of substellar objects (Crossfield, 2014). VizieR Online Data Catalog: J/A+A/566/A130. https://doi.org/10.26093/cds/vizier.35660130.

Getman, K. V., Broos, P. S., Kuhn, M. A., Feigelson, E. D., Richert, A. J. W., Ota, Y., Bate, M. R. and Garmire, G. P. (2017) Star formation in nearby clouds (SFiNCs): X-ray and infrared source catalogs and membership. ApJS, 229(2), 28. https://doi.org/10.3847/1538-4365/229/2/28.

Ghosh, S., Mondal, S., Dutta, S., Das, R., Joshi, S., Lata, S., Khata, D. and Panja, A. (2021) Fast photometric variability of very low mass stars in IC 348: detection of superflare in an M dwarf. MNRAS, 500(4), 5106–5116. https://doi.org/10.1093/mnras/staa3574.

Ilin, E. (2021) AltaiPony - flare science in Kepler, K2 and TESS light curves. JOSS, 6(62), 2845. https://doi.org/10.21105/joss.02845.

Lightkurve Collaboration, Cardoso, J. V. d. M., Hedges, C., Gully-Santiago, M., Saunders, N., Cody, A. M., Barclay, T., Hall, O., Sagear, S., Turtelboom, E., Zhang, J., Tzanidakis, A., Mighell, K., Coughlin, J., Bell, K., Berta-Thompson, Z., Williams, P., Dotson, J. and Barentsen, G. (2018) Lightkurve: Kepler and TESS time series analysis in Python. Astrophysics Source Code Library, record ascl:1812.013.

Lomb, N. R. (1976) Least-squares frequency analysis of unequally spaced data. Ap&SS, 39(2), 447–462. https://doi.org/10.1007/BF00648343.

Luhman, K. L., Esplin, T. L. and Loutrel, N. P. (2016) A census of young stars and brown dwarfs in IC 348 and NGC 1333. ApJ, 827(1), 52. https://doi.org/10.3847/0004-637X/827/1/52.

Luhman, K. L., Stauffer, J. R., Muench, A. A., Rieke, G. H., Lada, E. A., Bouvier, J. and Lada, C. J. (2003) A census of the young cluster IC 348. ApJ, 593(2), 1093–1115. https://doi.org/10.1086/376594.

Martín, E. L., Dougados, C., Magnier, E., Ménard, F., Magazzù, A., Cuillandre, J. C. and Delfosse, X. (2001) Four brown dwarfs in the Taurus star-forming region. ApJ, 561(2), L195–L198. https://doi.org/10.1086/324754.

Mohanty, S., Jayawardhana, R. and Basri, G. (2005) The T Tauri phase down to nearly planetary masses: Echelle spectra of 82 very low mass stars and brown dwarfs. ApJ, 626(1), 498–522. https://doi.org/10.1086/429794.

Palla, F. and Baraffe, I. (2005) Pulsating young brown dwarfs. A&A, 432(2), L57–L60. https://doi.org/10.1051/0004-6361:200500020.

Parker, R. J. and Alves de Oliveira, C. (2017) Dynamical histories of the IC 348 and NGC 1333 star-forming regions in Perseus. MNRAS, 468(4), 4340–4350. https://doi.org/10.1093/mnras/stx739.

Parks, J. R., Plavchan, P., White, R. J. and Gee, A. H. (2014) Periodic and aperiodic variability in the molecular cloud ρ Ophiuchus. ApJS, 211(1), 3. https://doi.org/10.1088/0067-0049/211/1/3.

Paudel, R. R., Gizis, J. E., Mullan, D. J., Schmidt, S. J., Burgasser, A. J., Williams, P. K. G. and Berger, E. (2018) *K2* ultracool dwarfs survey. IV. Monster flares observed on the young brown dwarf CFHT-BD-Tau 4. ApJ, 861(2), 76. https://doi.org/10.3847/1538-4357/aac8e0.

Rebull, L. M., Stauffer, J. R., Cody, A. M., Hillenbrand, L. A., Bouvier, J., Roggero, N. and David, T. J. (2020) Rotation of low-mass stars in Taurus with K2. AJ, 159(6), 273. https://doi.org/10.3847/1538-3881/ab893c.

Ricker, G. R., Winn, J. N., Vanderspek, R., Latham, D. W., Bakos, G. Á., Bean, J. L., Berta-Thompson, Z. K., Brown, T. M., Buchhave, L., Butler, N. R., Butler, R. P., Chaplin, W. J., Charbonneau, D., Christensen-Dalsgaard, J., Clampin, M., Deming, D., Doty, J., De Lee, N., Dressing, C., Dunham, E. W., Endl, M., Fressin, F., Ge, J., Henning, T., Holman, M. J., Howard, A. W., Ida, S., Jenkins, J. M., Jernigan, G., Johnson, J. A., Kaltenegger, L., Kawai, N., Kjeldsen, H., Laughlin, G., Levine, A. M., Lin, D., Lissauer, J. J., MacQueen, P., Marcy, G., McCullough, P. R., Morton, T. D., Narita, N., Paegert, M., Palle, E., Pepe, F., Pepper, J., Quirrenbach, A., Rinehart, S. A., Sasselov, D., Sato, B., Seager, S., Sozzetti, A., Stassun, K. G., Sullivan, P., Szentgyorgyi, A., Torres, G., Udry, S. and Villasenor, J. (2015) Transiting Exoplanet Survey Satellite (TESS). JATIS, 1, 014003. https://doi.org/10.1117/1.JATIS.1.1.014003.

Sagar, R., Naja, M., Maheswar, G. and Srivastava, A. K. (2014) Science at high-altitude sites of ARIES – astrophysics and atmospheric sciences. PINSA, 80, 759–790. https://doi.org/10.16943/ptinsa/2014/v80i4/55165.

Savitzky, A. and Golay, M. J. E. (1964) Smoothing and differentiation of data by simplified least squares procedures. AnaCh, 36(8), 1627–1639. https://doi.org/10.1021/ac60214a047.

Scargle, J. D. (1982) Studies in astronomical time series analysis. II. Statistical aspects of spectral analysis of unevenly spaced data. ApJ, 263, 835–853. https://doi.org/10.1086/160554.

Scholz, A. and Eislöffel, J. (2005) Rotation and variability of very low mass stars and brown dwarfs near ε Ori. A&A, 429, 1007–1023. https://doi.org/10.1051/0004-6361:20041932.

Scholz, A., Moore, K., Jayawardhana, R., Aigrain, S., Peterson, D. and Stelzer, B. (2018) A universal spin–mass relation for brown dwarfs and planets. ApJ, 859(2), 153. https://doi.org/10.3847/1538-4357/aabfbe.

Scholz, A., Xu, X., Jayawardhana, R., Wood, K., Eislöffel, J. and Quinn, C. (2009) Hotspots and a clumpy disc: variability of brown dwarfs and stars in the young σ Ori cluster. MNRAS, 398(2), 873–886. https://doi.org/10.1111/j.1365-2966.2009.15021.x.

Smith, J. C., Stumpe, M. C., Cleve, J. E. V., Jenkins, J. M., Barclay, T. S., Fanelli, M. N., Girouard, F. R., Kolodziejczak, J. J., McCauliff, S. D., Morris, R. L. and Twicken, J. D. (2012) *Kepler* presearch data conditioning II – A Bayesian approach to systematic error correction. PASP, 124(919), 1000–1014. https://doi.org/10.1086/667697.

Stumpe, M. C., Smith, J. C., Catanzarite, J. H., Cleve, J. E. V., Jenkins, J. M., Twicken, J. D. and Girouard, F. R. (2014) Multiscale systematic error correction via wavelet-based bandsplitting in kepler data. PASP, 126(935), 100–114. https://doi.org/10.1086/674989.

Toma, E. (1972) Pulsational instability of stars during deuterium burning. A&A, 19, 76–81.

VanderPlas, J. T. (2018) Understanding the Lomb-Scargle Periodogram. ApJS, 236(1), 16. https://doi.org/10.3847/1538-4365/aab766.